DOI: 10.18727/0722-6691/5266

Science Verification of CRIRES+

Bruno Leibundgut[1]
Mario van den Ancker[1]
Ben Courtney-Barrer[1]
Artie Hatzes[2]
Matias Jones[1]
Carlo F. Manara[1]
Paulo Miles Páez[1]
Florian Rodler[1]
Ditte Slumstrup[1]
Jonathan Smoker[1]
Elena Valenti[1]

[1] ESO
[2] Thüringer Landessternwarte Tautenburg, Germany

Science Verification (SV) observations with CRIRES+ were obtained between 15 and 19 September 2021. The SV team performed the observations jointly on Paranal and in Garching. The weather conditions were mostly good except for the last night when thick clouds prevailed for most of the night requiring adjustments for some observations. Most of the planned SV observing programme could be accomplished. Of 57 submitted proposals, 23 observing programmes were scheduled for a total of 47 hours of observations. The allocation assumed four observing nights (of ten hours each) and included a slight oversubscription. Sixteen projects could be completed, including the eight top priority programmes. Three programmes could only be partially executed, and four runs were not observed. Some of the first science results are presented.

Proposal solicitation and submission

The call for CRIRES+ SV proposals was issued on 16 June 2021[1]. With the call, the CRIRES+ SV Webpage[2] was launched. 57 proposals were received by the deadline on 7 July 2021 requesting in total 170 hours. The proposals were submitted through the regular P1 system in a special call. This is amongst the highest demands on recent instrument SVs. The SV team ranked the proposals according to scientific interest and the final selection was discussed at a meeting on 23 July 2021. 23 projects were selected for a total of 47 hours of execution time. Several proposals were rejected because they overlapped with submitted P108 proposals. One proposal requested time-critical observations outside the allocated SV nights and had to be rejected as well. The approved projects slightly oversubscribed the available time. The proposers were informed about the outcome of the selection on 3 August 2021. In parallel, the information was also made available to the Principal Investigators (PIs) through the Observing Programmes Office Webletter pages. The deadline for the submission of the Phase 2 material was 1 September 2021.

The largest number of requests were for exoplanet transit observations to characterise planetary atmospheres. Other topics included studies of circumstellar disc chemical composition, atomic gas in quasar absorption systems, obtaining the He isotope ratios towards the Orion Nebula, accretion and ejection of gas in discs around young stars, mass loss from post-red-supergiant stars, gas planets in the Solar System (Jupiter and Neptune), and abundance measurements in planetary nebulae and star clusters. Some of the first science results are presented below.

Observations

The CRIRES+ SV nights were scheduled for 15 to 19 September 2021. The schedule was determined by the CRIRES+ commissioning activities and had to remain flexible. In general, the atmospheric conditions were good except for high seeing during the first night and clouds during the last night. Observations could be obtained throughout the allocated CRIRES+ SV nights. In some cases, the observations had to be adjusted to the prevailing conditions and some data were obtained outside the requested observing constraints. CRIRES+ performed very well and only a small amount of time was lost for certain target acquisitions, caused by either crowded fields or mismatches in the filter/brightness combinations for the reference stars resulting in occasional deviations from the optimal observing schedule. No significant instrument problems were encountered during the four SV nights. The collaboration between the science operations on Paranal and the support team in Garching was excellent. A remote observing session from Garching was set up to train the CRIRES+ user support astronomers. There were very fruitful

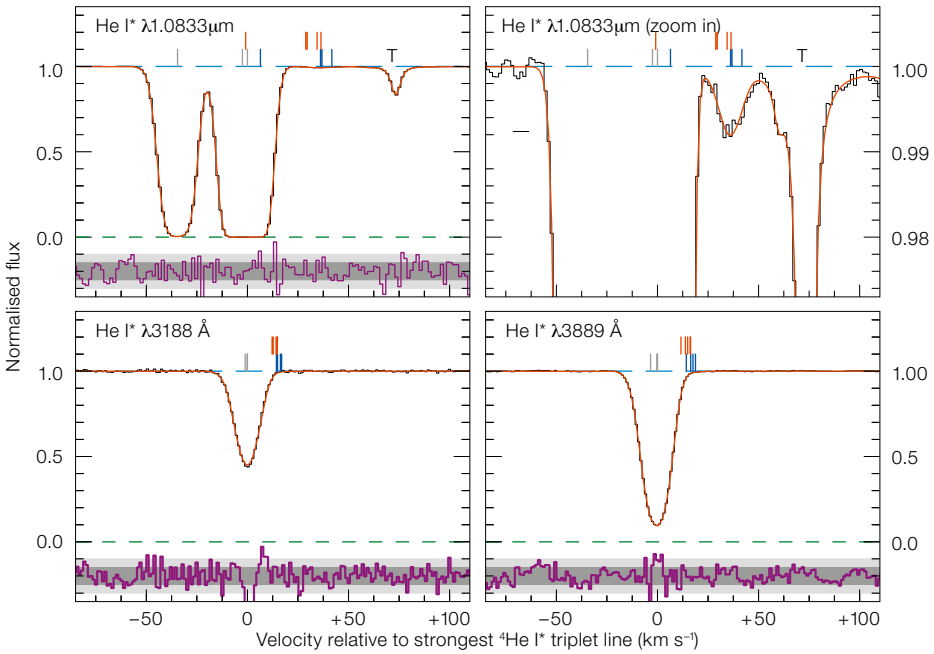

Figure 1. He I* absorption lines towards θ^2 A Ori. The top row shows the CRIRES+ observations and the bottom row archival data from the Ultraviolet and Visual Echelle Spectrograph (UVES). The ^{3}He I* lines are identified with the red and blue tick marks and are observed only in the CRIRES+ data. The grey tick marks indicate the positions of the ^{4}He I* lines and the 'T' marks a telluric line.

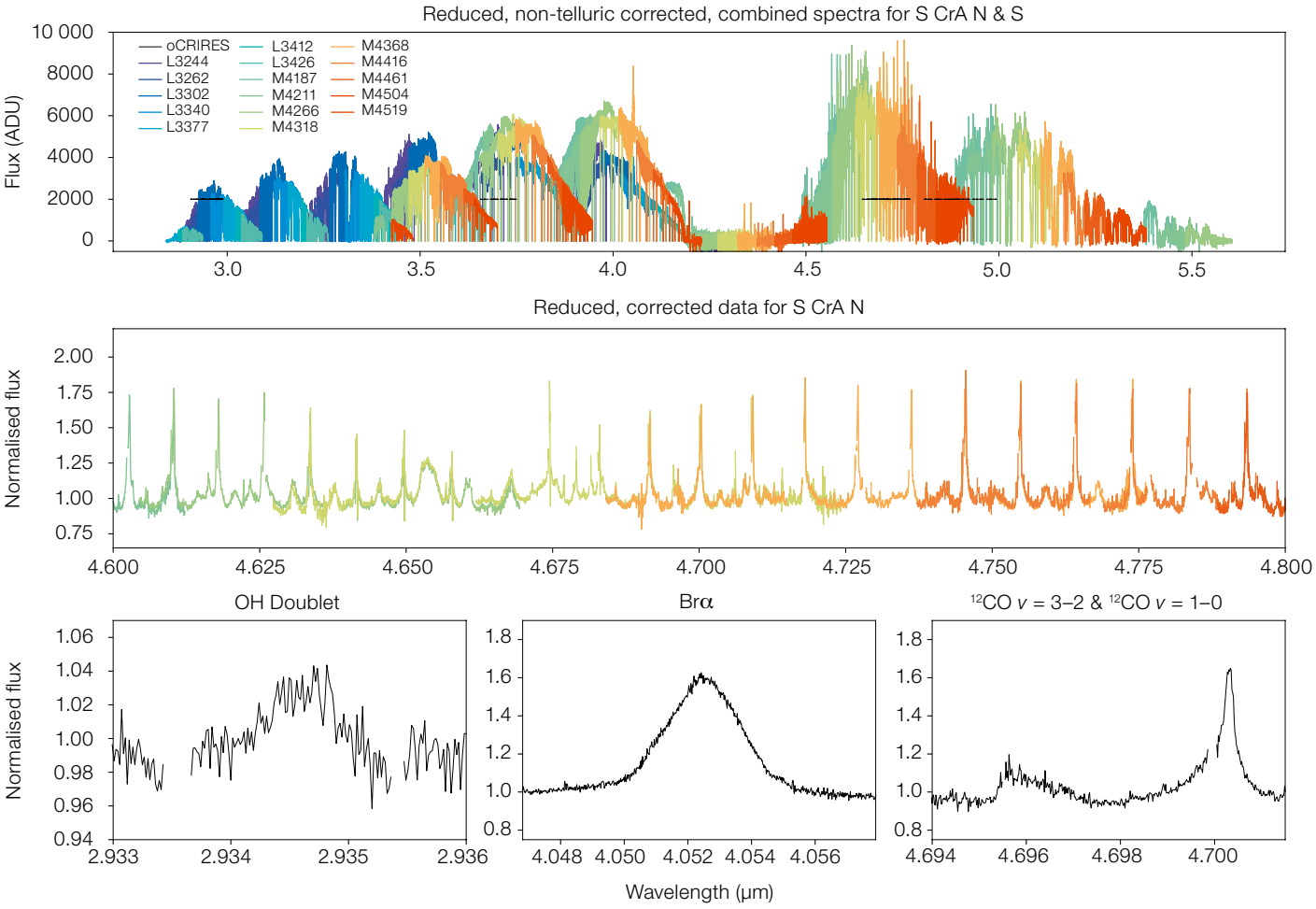

Figure 2. Top: The CRIRES+ pipeline reduced spectra for S CrA in all the *L*- and *M*-band settings. CRIRES data taken before the instrument upgrade as part of the ESO Large Programme 179.C-0151 are shown in black. Middle: The reduced and telluric-corrected spectra for S CrA N in a region rich with CO lines. Bottom: Examples of the spectral features seen in the data of S CrA N after combining any overlapping orders.

interactions between Paranal astronomers and Garching observers in regard to instrument operations.

Archive and data processing

All raw data are publicly available through the ESO science archive. The CRIRES+ SV webpage has been updated with direct links to the raw data in the archive. The preliminary version of the CRIRES+ data reduction pipeline was made available to the PIs through the notification notes they received shortly after the observations were obtained. In the meantime the CRIRES+ pipeline was released with the start of operations at the beginning of October 2021 and the link is provided through the CRIRES+ SV webpage as well.

First science results

Several PIs of successful CRIRES+ SV programmes very kindly shared their first results for presentation in this article. In some cases, manuscripts have already been submitted for publication.

Primordial ^{3}He

A brief period of nucleosynthesis, a few minutes after the Big Bang, created five nuclides in abundance. The relative abundance of these primordial nuclides provides our earliest probe of fundamental physics and cosmology. Historically, the most challenging of these nuclides to measure has been Helium-3 (^{3}He) and it has so far only been detected in the Milky Way. CRIRES+ was used to secure the first measurement of the helium isotope ratio (^{3}He/^{4}He) beyond the Local Interstellar Cloud. This is based on the observation of a meta-stable helium absorption seen against a bright star in the Orion Nebula (θ^2 A Ori). This measurement requires high spectral resolution data with an extremely high signal-to-noise ratio (S/N). A precise value of ^{3}He/^{4}He = (1.77 ± 0.13) × 10^{-4} was determined, which is just ~ 40 per cent above the primordial relative abundance of these isotopes, assuming the Standard Model of particle physics and cosmology, of ^{3}He/^{4}He$_p$ = (1.257 ± 0.017) × 10^{-4}. This novel measurement technique offers a

new opportunity to study the physics of the early Universe, and the potential to detect ^{3}He in a more primitive environment beyond the Milky Way.

Protoplanetary disc composition

High spectral resolution *L*- and *M*-band observations offer a unique probe into the kinematics, structure, and composition of the inner 10 astronomical units (au) of protoplanetary discs. A full spectral scan of the binary system S Coronae Australis (S CrA) in the *L* and *M* bands was observed with CRIRES$^+$. These observations tested the new spectral coverage of CRIRES$^+$ on a target that had been observed with CRIRES prior to its upgrade (Pontoppidan, Blake, & Smette, 2011; Pontoppidan et al., 2011; Brown et al., 2013; Banzatti et al., 2017). The full spectral scan provides complete coverage from 2.9 to 5.5 µm and the overlap of orders from different filters gives a unique opportunity to test which settings provide the highest quality data at a given wavelength. Spectral lines from H_2O, OH, HCN, and CO all fall within the coverage, along with several atomic hydrogen lines. This is the first complete high-resolution *L*- and *M*-band spectrum of any protoplanetary disc obtained to date.

CO disc

Most of our knowledge about the physical properties of protoplanetary discs is based on studies of the dusty disc beyond ~1–2 au. Very little is known about the innermost disc. Probing the inner disc is key as it can provide insights into the processes driving evolution and disc dissipation, as well as the initial conditions for planets forming in short orbits. One of the few observational probes of the innermost disc is the overtone emission of CO at 2.3–2.5 µm (for example, GRAVITY Collaboration, 2021). CRIRES$^+$ observations of the CO bandhead in the Herbig Ae/Be star HD 36917 characterise the properties of the gas emitting the CO bandheads. By modelling the spectrum with a CO disc model, physical properties of the CO emitting gas (temperature and CO density) and its kinematics (for example, rotational velocity) can be derived. The intrinsic line widths of the individual J-components are determined, which potentially constrain the angular momentum transport. Important information about the physics of the inner gaseous disc, for which no model is currently available, can be obtained.

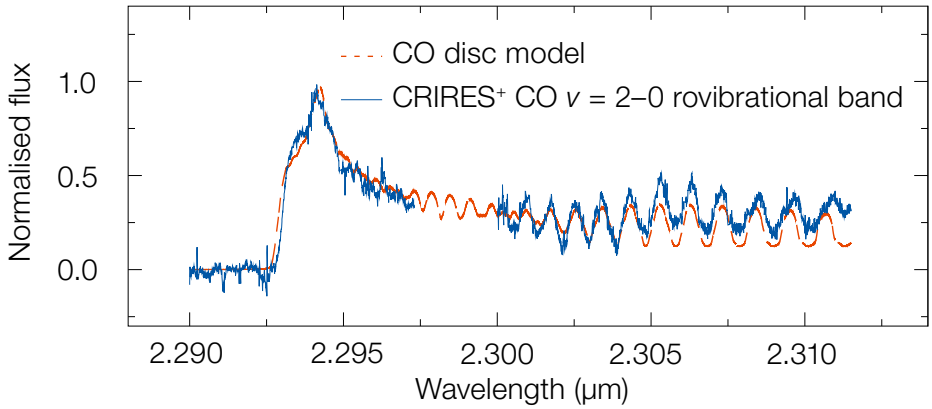

Figure 3. CRIRES$^+$ spectrum of the first CO overtone emission of the Herbig Ae star HD 36917 (blue spectrum). The spectrum is continuum subtracted and normalised to the peak of the bandhead. Preliminary results of a CO model are over-plotted as a red dashed line. The CO is modelled as a disc in Keplerian rotation at a temperature T = 3000 K, a CO column density of 3 × 10^{21} cm^{-2}, intrinsic line width of 0.5 km s^{-1}, and v_{rot} sin(i) ≈ 113 km s^{-1}. The CO emitting disc extends from around 0.3 au to 2 au from the central source.

Alpha-enhanced star in the Galactic centre

The Nuclear Star Cluster (NSC) lies behind 30 magnitudes of optical extinction at the centre of the Milky Way. This compact

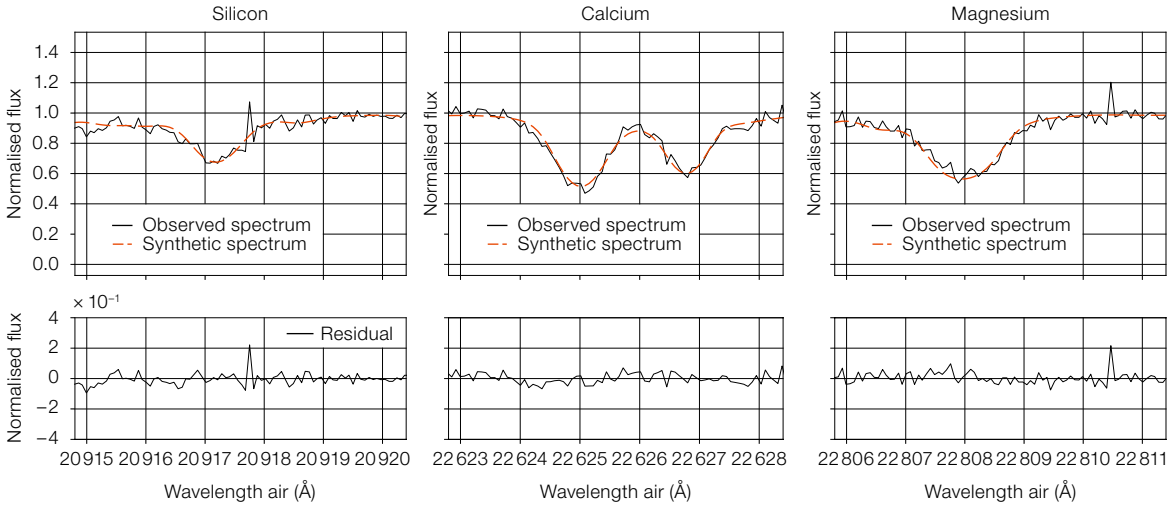

Figure 4. Synthetic spectrum showing the goodness of fit for three α-elements, namely Si, Ca and Mg. The synthetic spectrum was generated using the stellar parameters from Thorsbro et al. (2020).

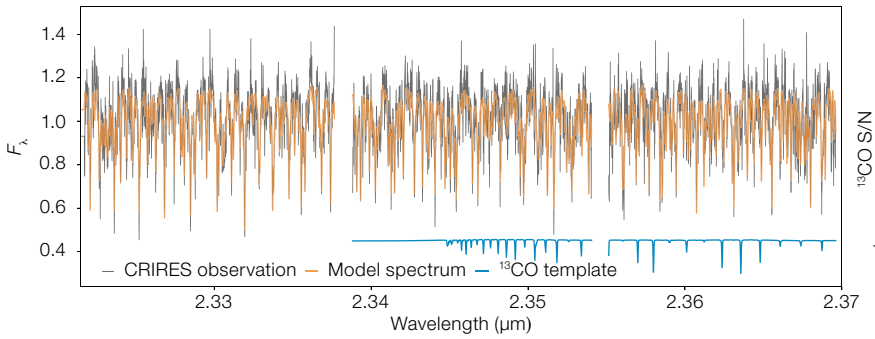

Figure 5. CO lines in a brown dwarf spectrum. Left panel: The CRIRES+ data are shown in black, the model in orange, and the positions of the ^{13}CO lines are indicated in blue (left panel). Right panel: The detection of the ^{13}CO lines.

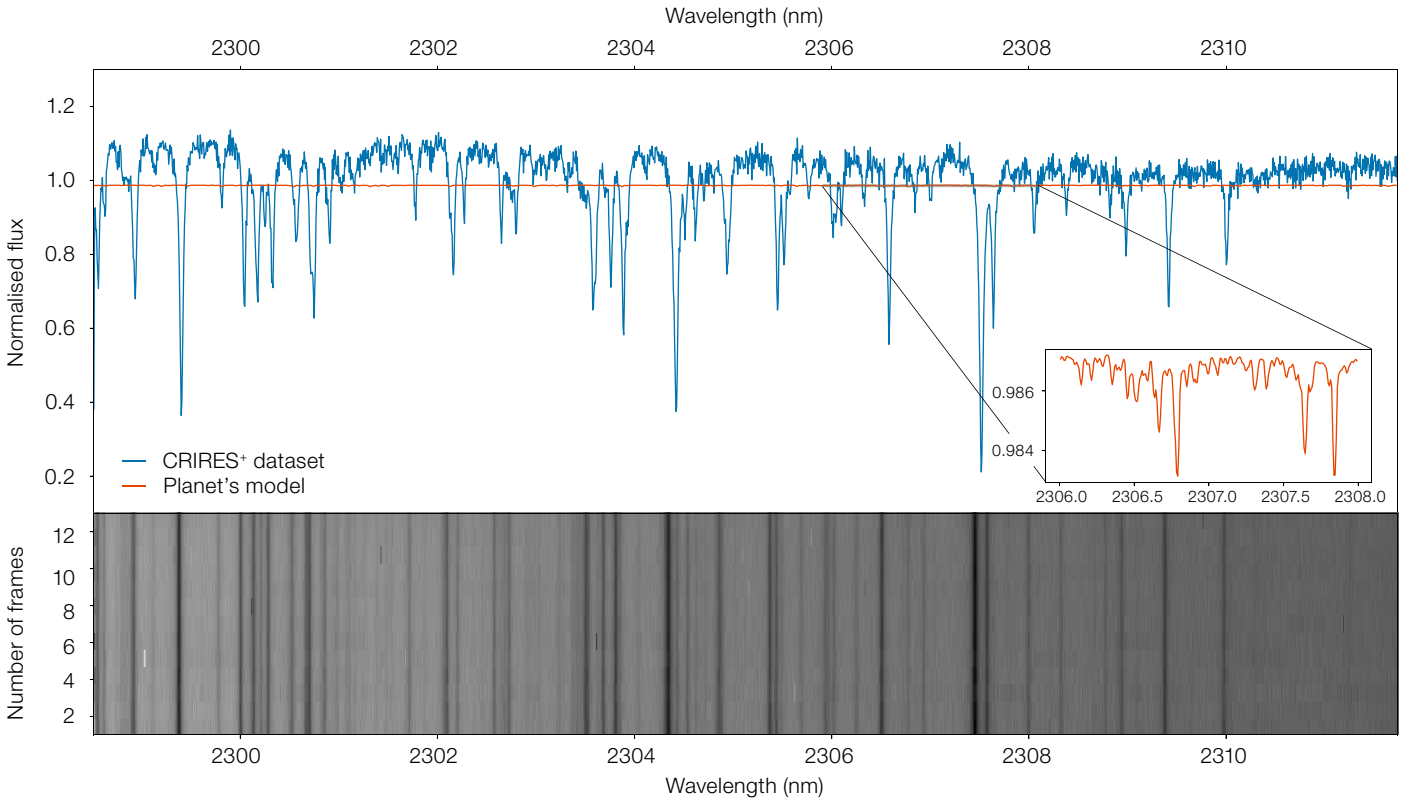

Figure 6. Example of extracted spectrum of Wasp-20b with the CRIRES+ pipeline. Top: Comparison between the raw dataset (blue line) and a synthetic spectrum of Wasp-20b (red line), obtained from a 1D model. Small box: Zoom of a section of the planet's spectrum. The signal of the planet is completely drowned by the telluric absorption, the stellar signal and the instrumental noise, which are still present in the raw dataset and are hundreds of times stronger. Bottom: Consecutive frames of the same spectrum are ordered along the y-axis. The strongest contaminating signals (i.e., telluric absorption and stellar signal) occur always at the same wavelength, resulting in straight black lines.

structure, with an effective radius of about 4 pc, consists of several million stars, appears to be very old (> 10 Gyr), and contains very metal rich stars. The formation history of the NSC is an open question. It could be the surviving core of multiple globular clusters or parts could be formed in situ and/or contain stars that have migrated from the inner Milky Way disc.

A star in the NSC was observed with CRIRES+ in the *K* band using the K2192 setting with a 0.2-arcsecond slit width (R ~ 100 000). The star had previously been observed with the NIRSPEC spectrograph on the KECK II telescope (Thorsbro et al., 2020) with R ~ 23 000. That observation determined stellar parameters of $T_{\rm eff}$ = 3359 ± 150 K, log g = 0.64±0.3, and [Fe/H] = 0.25±0.15. The preliminary reductions of the CRIRES+ observation confirm these parameters. Thorsbro et al. (2020) find a silicon abundance for the star at [Si/Fe] = 0.25 ± 0.15, which is remarkable as [Si/Fe] ~ 0.10 ± 0.15 for local disc stars, suggesting that at least silicon could be enhanced for NSC stars. The CRIRES+ preliminary results indicate [Si/Fe] = 0.20 ± 0.10, [Ca/Fe] = 0.20 ± 0.10, and [Mg/Fe] = 0.15 ± 0.10. This yields an average for α-elements close to 0.20. The CRIRES+ data strengthen the evidence for enhanced α-elements.

Brown dwarf spectrum

CRIRES$^+$ provides a great opportunity to link atmospheric characterisation to the formation history of exoplanets and brown dwarfs. The high spectral resolving power of CRIRES$^+$ facilitates the search for isotopologue features in emission spectra of planetary-mass objects. A *K*-band spectrum of the low-mass, young brown dwarf 2MASS J03552337+1133437 was obtained with a half-hour observation at a spectral resolution of $R \sim 80\,000$. The spectrum is shown as a black line in Figure 5 (left panel). The isotopologue ^{13}CO is detected at S/N ~ 6.5 (right panel) through the cross-correlation between the observation and the ^{13}CO template. A retrieval analysis was performed to generate the best-fit model spectrum (orange line) and constrain atmospheric properties of the L dwarf, in particular the carbon-to-oxygen abundance ratio, and the C and O isotope ratio in the atmosphere, which are potential probes of formation pathways of planets and brown dwarfs (Zhang et al., 2021; Zhang, Snellen & Mollière, 2021). In the future, analyses such as presented here can be conducted on a wide range of planetary-mass objects to unveil planet formation history.

Exoplanet spectra

The transit of WASP-20b, a hot Saturn planet, was observed for five hours on 16 September 2021. The planet has an equilibrium temperature close to 1400 K and orbits its host star in less than 5 days. The calibration and extraction of spectra were performed with the new CRIRES$^+$ pipeline, but at this point of the analysis the planetary spectrum is still completely hidden by the stellar signal and the telluric lines. A direct comparison is given in the top panel of Figure 6, where one of the extracted spectra (blue line) is over-plotted onto a synthetic spectrum of Wasp-20b (red line), obtained from a 1D model. The amplitude of the synthetic spectrum is many times smaller than the observed spectrum, which is dominated by telluric features.

Contrary to the planet's signal, which undergoes larger Doppler shifts during the night, the contaminators are stationary or quasi-stationary, which means that they always occur at the same wavelength. Figure 6 (bottom panel) displays the spectra from different observations ordered by time along the y-axis. The stable telluric and stellar features result in straight black lines. A principal component analysis is used to separate the velocity shifts and to disentangle the spectrum of the planet from all the other signals so as to detect molecular features in its atmosphere.

A second observation concerned the exoplanet system MASCARA-1b (Talens et al., 2017). It was observed with CRIRES$^+$ during a transit from phase ≈ 0.33 to 0.42, with 107 exposures (where phase = 0 and phase = 0.5 correspond to central transit and secondary eclipse, respectively). The goal was to detect C+O-bearing molecular species using Doppler-resolved cross-correlation spectroscopy (Snellen et al., 2010). This works by first removing the stellar and telluric lines from the data, and then cross-correlating the 'residual' spectra with spectral templates containing the signal of interest, in this example H_2O (resulting in cross-correlation functions as a function of v_{sys}). The cross-correlation signals are then summed as a function of time, assuming a range of values for the planetary velocity amplitude K_p.

The CRIRES$^+$ pipeline was used to extract 'raw' spectra for each spectral order as a function of time. These spectra are shown in the upper plot of Figure 7, before performing some standard pre-processing (including outlier rejection and blaze correction — middle panel of Figure 7). The SysRem algorithm (Tamuz, Mazeh & Zucker, 2005) was employed to remove the stellar and telluric lines (bottom panel of Figure 7) and to generate a planetary template spectrum assuming only H_2O in the atmosphere. The spectra were then cross-correlated with the template spectrum (over a velocity range of –150 to 150 km s^{-1}), before being summed over the planetary velocity for a range of K_p (from –300 to 300 km s^{-1}). The detection significance was then determined by dividing through the K_p v_{sys} map by the noise (after excluding regions around the peak and near $K_p = 0$). We found a peak detection of > 4σ near the expected K_p

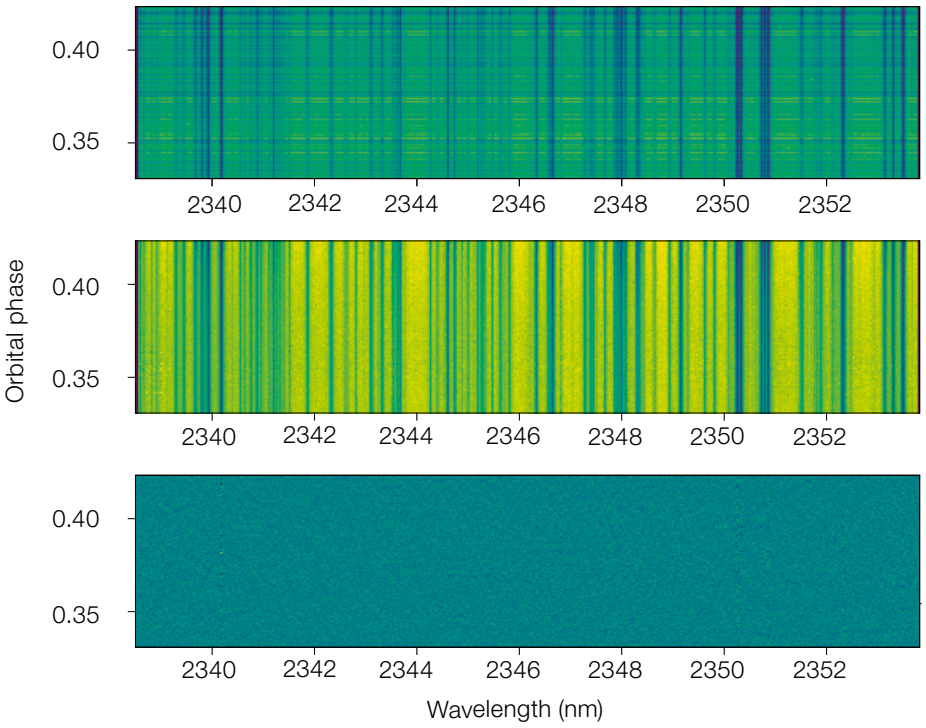

Figure 7. Top panel: Raw spectra for a single CRIRES$^+$ order as a function of time/orbital phase. Middle panel: Spectra after initial pre-processing including blaze correction. Bottom panel: Final 'residual' spectra after removing the telluric features using SysRem.

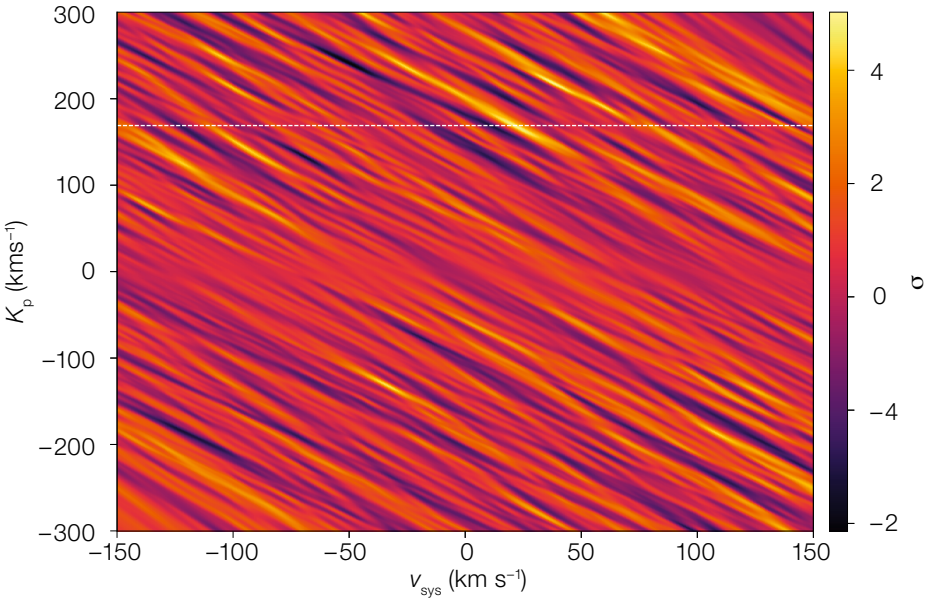

Figure 8. K_p–v_{sys} map of the of the summed cross-correlation signal for a H_2O template. The plot shows a tentative detection of water near the expected K_p and v_{sys} at > 4σ; however, refinements of the model templates are continuing in order to confirm the signal.

and v_{sys} indicating the probable detection of water. Further work is required to confirm the signal, as well as to search for other molecular species. See Gibson et al. (2020, 2022) for further details of the data processing and model templates.

Radial velocity of an exoplanet host star

Hot Jupiters are gaseous giant planets, orbiting their host stars in tight orbits at typical distances of a few percent of an au. The formation and evolution processes of hot Jupiters remain under debate. It is thought that these planets form at large orbital distances beyond the snowline, much like the Solar System giants, and subsequently undergo inward migration via disc–planet interaction or, alternatively, dynamical planet–planet scattering or star–planet interactions via the Kozai–Lidov mechanism (Kozai, 1962; Lidov, 1962). These mechanisms produce systems with distinct distributions of the alignment of stellar rotational axis and planetary orbit normal.

HIP 65Ab is an extreme hot Jupiter. With a mass of 3.2 M_{Jup}, it orbits its K4-type host star in an exceptionally short 0.98-day orbit, yielding a grazing transit geometry, potentially indicative of an oblique orbit (Nielsen et al., 2020). While in transiting systems the planetary radius can be determined via photometric transit light curves, radial velocity (RV) measurements of the stellar reflex motion remain indispensable for determining the planetary mass; by means of the Rossiter–McLaughlin effect (Rossiter, 1924; McLaughlin, 1924) the orbit obliquity can also be measured.

A spectral transit time series of HIP 65Ab was obtained to measure the stellar reflex motion and potentially the Rossiter–McLaughlin effect in HIP 65A in the *K* band. The observations cover a complete planetary transit, lasting only 45 minutes, and take advantage of the absorption gas-cell installed in CRIRES+ serving as a reference standard for RV measurements. RV measurements were obtained using the VIPER pipeline (Zechmeister, Köhler & Charmathi, 2021). The observations suffered from adverse weather conditions (thick clouds) which caused strong interference by telluric lines and prevented the requested adaptive optics operations, resulting in a severely

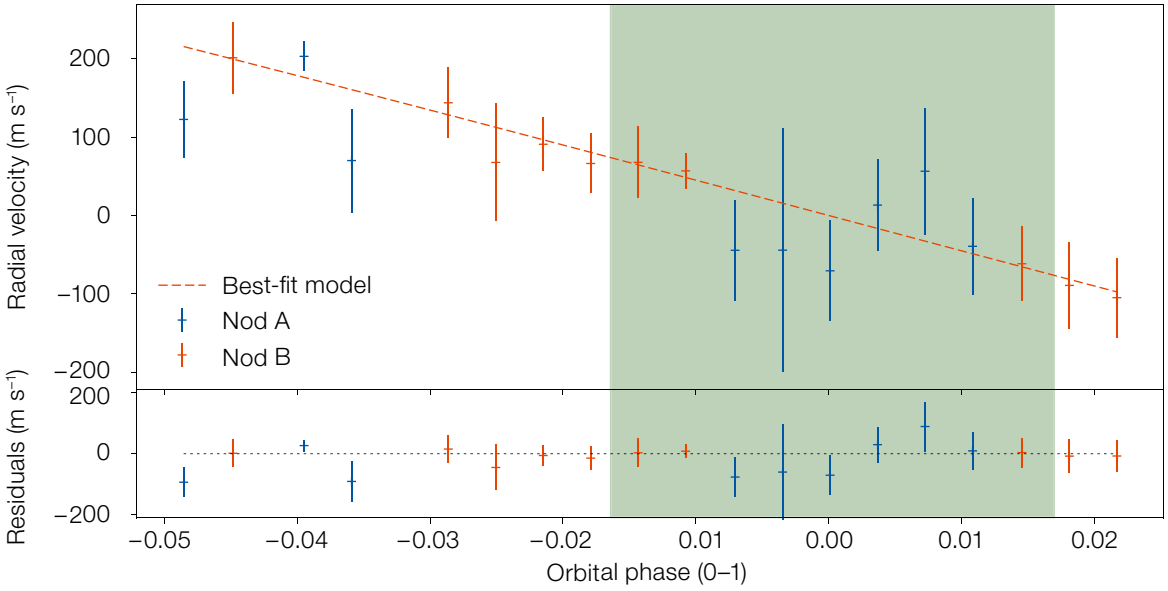

Figure 9. Radial velocity change of the host star HIP 65A during a planetary transit. The green area indicates first and fourth contact.

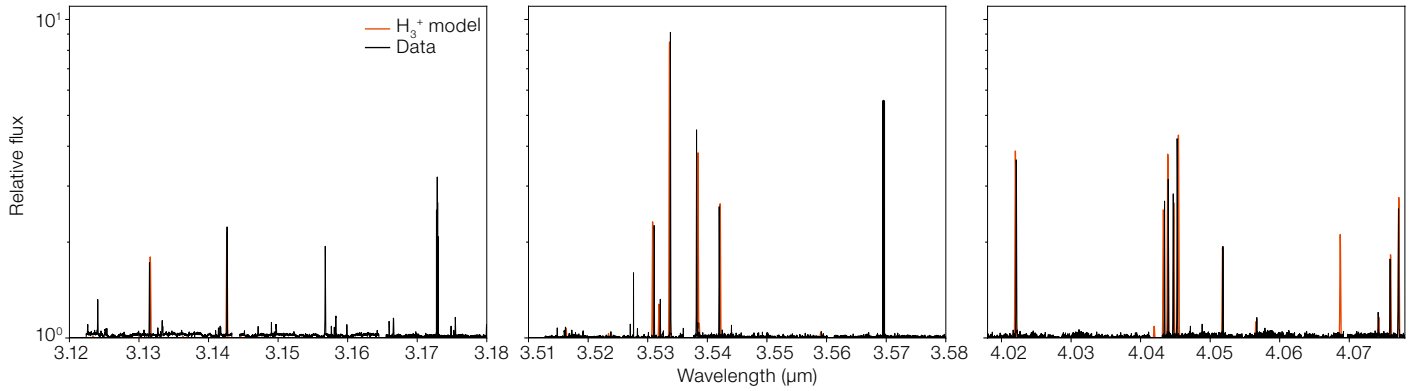

Figure 10. Selected wavelength regions of CRIRES$^+$ data from Jupiter's auroral region (black). A large number of emission lines from H_3^+ are clearly visible. A model based on the linelist from Neale, Miller & Tennyson (1996) is shown for comparison (red).

diminished S/N of the spectra. While this prevents a meaningful analysis of the Rossiter–McLaughlin effect, the result clearly shows the stellar reflex motion of HIP 65A (Figure 9) corresponding to a RV semi-amplitude of 715 ± 90 ms^{-1} determined with CRIRES$^+$ alone.

Neptune

Neptune was observed on 19 September 2021 in selected spectral regions between 1.48 μm and 5.15 μm. The goal was to assess Neptune's atmospheric composition and to better constrain emission from carbon monoxide (CO) and the trihydrogen cation (H_3^+) in the upper atmosphere and absorption from methane near the tropopause. The adaptive optics system was unable to lock on to the extended disc of Neptune, resulting in seeing between 0.28 and 0.77 arcseconds. Thick clouds also moved in during the observations, reducing the sky transparency and data quality.

The CRIRES$^+$ spectra resolve Neptune's ~2.3-arcsecond-diameter disc. In the *H* band, (1.582 μm central wavelength), brightness variations across the disc are seen with a distinctly greater radiance along the northern edge of the planet. Spatial variation across the disc is particularly evident between 1.52 μm and 1.64 μm where methane absorption is weakest. With increasing wavelength, the disc grows fainter. This behaviour suggests that there is a significant difference in the altitude of the highest clouds between the south and north. This is likely due to scattering from a discrete cloud near the tropopause in Neptune's northern hemisphere. In the *K* band, scattering from the bright northern regions extends to wavelengths < 2.15 μm, but no signal is evident from most of the disc. This discrete reflectance declines in intensity with increasing wavelength, with no signal evident between 2.15 μm and 2.48 μm. This is consistent with sunlight scattered by the high-altitude clouds becoming increasingly attenuated by molecular hydrogen collisional-induced absorption (CIA). Some signal is observed again between 2.48 μm and 2.53 μm, where H_2-CIA is reduced. Careful analysis of the reflectance *K* band and *H* bands together will be used to potentially constrain the methane abundance near Neptune's tropopause (Roman, Banfield & Gierasch, 2018).

Only a very faint signal is observed in the *L* band at the shortest wavelengths (≤ 2.9 μm). No obvious H_3^+ lines are detected. There appears to be a faint, indistinct planetary signal across much of the raw spectrum in the *M* band. The radiances appear rather flat and featureless, which may be the result of a combination of thermal emission and scattering from Neptune's upper troposphere. There is no obvious evidence of the 4.7 μm CO fluorescence feature previously detected in AKARI satellite spectra (Fletcher et al., 2010). If the CO fluorescence is indeed now absent, it may be indicative of temporal changes in the CO abundance or solar activity. However, the telluric absorption and emission are very prominent at these wavelengths, and further work is needed to improve the reduction and calibration for analysis.

Jupiter

Auroral H_3^+ line emission was first observed in 1989 in Jupiter and since then detected in Saturn and Uranus. It is a prominent indicator for auroral geometry and a sensitive probe of the planetary atmosphere and magnetosphere, and it plays an important role in the dynamics, heating, cooling and chemistry of the Solar System planets. The data will provide a benchmark for future research in Solar System planetary atmospheres and for the search for H_3^+ in exoplanets. H_3^+ spectroscopy provides new opportunities for characterising exoplanet atmospheres from ground-based observatories and in non-transiting planets.

Hydrogen Brackett and Pfund series in supergiant stars

Two rare, massive post-red-supergiants, IRAS 17163-3907 and IRC+10420 (Koumpia et al., 2020; Oudmaijer & de Wit, 2013), were observed in the *M* band at four different settings (M4416, M4368, M4318, M4266). All settings combined provide a very good wavelength coverage between 3.4 and 5.3 μm. These observations make it possible to probe powerful hydrogen diagnostic lines of the Bracket and Pfund series of hydrogen, as well as the CO (v = 1-0) rovibrational transitions (see Figure 11). The emission lines probe material originating in a region at typically thousands of kelvin, while absorption occurs in cooler regions, at several hundred kelvin. Both are present in the spec-

trum of IRC+10420, which in addition shows P-Cygni signatures in its CO emitting gas, indicative of an expansion. This is the first time IRAS 17163-390 has been observed spectroscopically in the *M* band, which besides its extreme spectral similarities to IRC+10420 at shorter wavelengths, appears to show generally stronger hydrogen recombination lines, but weaker CO absorption. The very high spectral resolution, of order 80 000, will permit the authors to derive the velocity of the outflowing material, and also to determine the temperatures and densities of the regions where mass-loss takes place using LTE and non-LTE radiative transfer modelling. The wind/outflow velocity distribution traced with the warm CO emission will constrain the outflow velocity very close to the yellow hypergiant and therefore the most recent mass-loss rates and kinematic timescales.

Conclusions

CRIRES+ SV can be considered a success. The scientific results presented are an initial sample of the science CRIRES+ will address in the future. It will be an excellent tool with which to examine and characterise exoplanet atmospheres, stellar discs and stars. The instrument is now in full operation.

Acknowledgements

We thank the many scientists who have prepared the preliminary results presented in this article. They are Ryan Cooke, Pasquier Noterdaeme, James Johnson, Louise Welsh, Max Pettini, Céline Péroux, Michael Murphy, David Weinberg, Brian Thorsbro, Alexis Lavail, Nils Ryde, Maria Chiara Maimone, Andrea Chiavassa, Matteo Brogi, Yapeng Zhang, Ignas Snellen, Jayne Birkby, Evangelos Nagel, Stefan Czesla, Ulf Seeman, Jana Köhler, Evgenia Koumpia, René Oudmaijer, Sierra Grant, Arthur Bosman, Giulio Bettoni, Andrea Banzatti, Rebecca García López, Antonella Natta, Alessio Caratti o Garatti, David Hollenbach, Uma Gorti, Michael Roman, Leigh Fletcher, Ansgar Reiners, Jan Klimke, Lisa Nortmann, Joachim Sauer, Neale Gibson, Swaetha Ramkumar, Stevanus Nugroho, Cathal Gallagher.

References

Banzatti, A. et al. 2017, ApJ, 834, 152
Brown, J. M. et al. 2013, ApJ, 770, 94
Fletcher, L. N. et al. 2010, A&A, 514, A17
Gibson, N. P. et al. 2020, MNRAS, 493, 2215
Gibson, N. P. et al. 2022, MNRAS, in press, arXiv:2201.04025

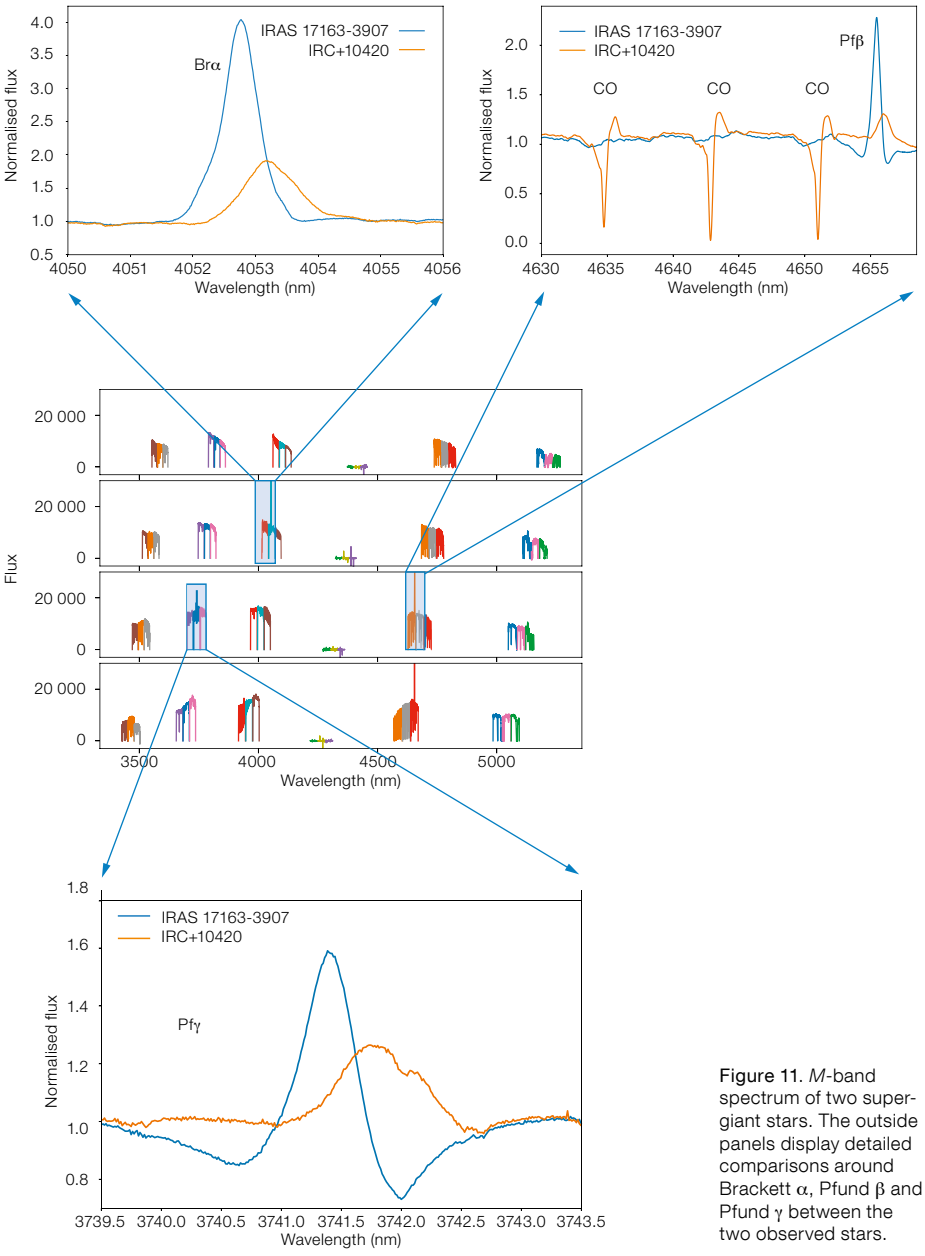

Figure 11. *M*-band spectrum of two supergiant stars. The outside panels display detailed comparisons around Brackett α, Pfund β and Pfund γ between the two observed stars.

GRAVITY Collaboration 2021, A&A, 645, A50
Koumpia, E. et al. 2020, A&A, 635, A183
Kozai, Y. 1962, AJ, 67, 591
Lidov, M. L. 1962, Planet. Space Sci., 9, 719
McLaughlin, D. B. 1924, ApJ, 60, 22
Neale, L., Miller, S. & Tennyson, J. 1996, ApJ, 464, 516
Nielsen, L. D. et al. 2020, A&A, 639, A76
Oudmaijer, R. D. & de Wit, W. J. 2013, A&A, 551, A69
Pontoppidan, K. M., Blake, G. A. & Smette, A. 2011, ApJ, 733, 84
Pontoppidan, K. M. et al. 2011, The Messenger, 143, 32
Roman, M. T., Banfield, D. & Gierasch, P. J. 2018, Icarus, 310, 54
Rossiter, R. A. 1924, ApJ, 69, 15
Snellen, I. et al. 2010, Nature, 465, 1049
Talens, G. J. J. et al. 2017, A&A, 606, A73
Tamuz, O., Mazeh, T. & Zucker, S. 2005, MNRAS, 356, 1466
Thorsbro, B. et al. 2020, ApJ, 894, 26
Zechmeister, M., Köhler, J. & Charmathi, S. 2021, Astrophysics Source Code Library, 2108.006
Zhang, Y. et al. 2021, Nature, 595, 370
Zhang, Y., Snellen, I. A. G. & Mollière, P. 2021, A&A, 656, A76

Links

[1] Call for CRIRES+ SV proposals: https://www.eso.org/sci/publications/announcements/sciann17414.html
[2] CRIRES+ SV: http://www.eso.org/sci/activities/vltsv/criresplussv.html